

# X-ray and optical variability of the ultraluminous X-ray source NGC 1313 X-2

P. Mucciarelli<sup>1,2</sup>, L. Zampieri<sup>2</sup>, A. Treves<sup>3</sup>, R. Turolla<sup>4</sup> and R. Falomo<sup>2</sup>

## ABSTRACT

We present an analysis of recent *XMM-Newton* and *HST* archive data of the ultraluminous X-ray source NGC 1313 X-2. Quasi-simultaneous observations taken with *XMM-Newton*, *HST* and VLT allow us to study both the X-ray light curve and its correlation with the optical emission of the two proposed ULX counterparts. At the end of December 2003 the source experienced a short, but intense flare, reaching a maximum luminosity of  $\sim 10^{40}$  erg/s. At the same time, the optical flux of both the suggested counterparts did not show pronounced variations ( $\lesssim 30\%$ ). Assuming that the ULX emission is isotropic and taking X-ray reprocessing into account, the optical data for one of the proposed counterparts are consistent with it being an early type, main sequence star of  $\sim 10 - 18M_{\odot}$  losing matter through Roche-lobe overflow onto a  $\sim 120M_{\odot}$  black hole at an orbital separation corresponding to a period of  $\sim 2$  days.

*Subject headings:* galaxies: individual (NGC 1313) — stars: individual (NGC 1313 X-2) — X-rays: binaries — X-rays: galaxies

## 1. Introduction

When, at the beginning of the 1980s, point-like, off-nuclear X-ray sources in the field of nearby galaxies were first detected (see, e.g., Fabbiano 1989), it was immediately recognized that their luminosity was unusually large. If physically associated with their host galaxies,

---

<sup>1</sup>Department of Astronomy, University of Padova, Vicolo dell'Osservatorio 2, I-35122 Padova, Italy; paola.mucciarelli@oapd.inaf.it

<sup>2</sup>INAF-Astronomical Observatory of Padova, Vicolo dell'Osservatorio 5, I-35122 Padova, Italy; zampieri@pd.astro.it, falomo@pd.astro.it

<sup>3</sup>Department of Physics and Mathematics, University of Insubria, Via Valleggio 11, I-22100 Como, Italy; treves@mib.infn.it

<sup>4</sup>Department of Physics, University of Padova, Via Marzolo 8, I-35131 Padova, Italy; turolla@pd.infn.it

these sources would have an isotropic luminosity in excess of the Eddington limit for a  $10M_{\odot}$  object. Nowadays, more than 150 ultraluminous X-ray sources (ULXs) are known (see e.g. Roberts & Warwick 2000; Colbert & Ptak 2002; Swartz et al. 2004; Liu & Bregman 2005).

It is estimated that a significant fraction of ULXs are interacting supernovae or background AGNs ( $\sim 50\%$ ; see Foschini et al. 2002b; Masetti et al. 2003; Swartz et al. 2004). However, the X-ray variability of many of them is similar to that observed in Galactic X-ray binaries (see e.g. La Parola et al. 2001; Colbert & Ptak 2002; Swartz et al. 2004; Zampieri et al. 2004, hereafter Z04). The recent detection of a 62 days modulation in the light curve of M 82 X-1, interpreted as the orbital period of the system, provided a direct confirmation of the binary nature of at least some ULXs (Kaaret, Simet & Lang 2006a,b). Moreover, ULX spectral properties share similarities with those of Galactic black hole X-ray binaries (BHXRBS, e.g. Foschini et al. 2002a). In several cases the spectrum can be well reproduced by a multicolor disk (MCD) blackbody plus a power law (PL), although the temperature of the MCD component is often much lower than that observed in BHXRBS (e.g. Miller et al. 2003, 2004; Feng & Kaaret 2005). For the brightest ULXs, a possible curvature above 2-3 keV has been recently reported and more sophisticated spectral models appear to give better agreement with observations (Stobbart et al. 2006).

All these properties along, in some cases, with the detection of stellar-like optical counterparts (Roberts et al. 2001; Goad et al. 2002; Liu et al. 2002, 2004; Kaaret et al. 2004; Z04; Kaaret 2005; Mucciarelli et al. 2005, hereafter M05; Soria et al. 2005), strongly suggest that a sizeable fraction of ULXs are accreting X-ray binaries. The present debate is focussed on understanding what type of binaries they are. Many of the ULX properties can be explained if they do not emit isotropically (King et al. 2001; King 2002; King & Pounds 2003) or are dominated by emission from a relativistic jet (Körding et al. 2002; Georganopoulos et al. 2002; Kaaret et al. 2003). Another possibility is that they are truly emitting above the Eddington limit for  $10M_{\odot}$ , either because accretion proceeds through a slim disk (Ebisawa et al. 2003; Kawaguchi 2003) or because the compact object is an Intermediate Mass Black Hole (IMBH) with a mass in excess of  $100M_{\odot}$  (e.g. Colbert & Mushotzky 1999; Miller et al. 2003; Patruno et al. 2005, 2006). Despite the inherent difficulties due to the low counting statistics, X-ray timing analysis has been attempted in some ULXs and led to the detection of a quasi periodic oscillation in the power density spectrum of M 82 X-1. This may represent a powerful, independent method to measure the black hole mass (Strohmayer & Mushotzky 2003; Fiorito & Titarchuk 2004; Dewangan et al. 2006; Mucciarelli et al. 2006).

Multiwavelength observations are an invaluable tool to investigate the nature of ULXs. Radio emission, when present, gives important clues about the geometry, energetics and lifetime of ULXs (Kaaret et al. 2003; Miller et al. 2005). Optical observations are crucial

to identify ULX counterparts and to study the properties of putative ULX binary systems. Up to now only a very small number of ULXs have been convincingly associated with stellar objects of known spectral type (e.g. Liu et al 2002, 2004; Kaaret et al. 2004; M05). All these ULXs are hosted in young stellar environments or star-forming regions and their optical counterparts have properties consistent with those of massive stars. Some ULXs are also associated with extended optical emission nebulae (Pakull & Mirioni 2002; Pakull, Grisé & Motch 2006).

NGC 1313 X-2 is a well studied ULX. The X-ray variability, high (isotropic) luminosity and presence of a soft X-ray spectral component make it a prototypical object. Furthermore, the presence of an emission nebula (Pakull & Mirioni 2002; Ramsey et al. 2006; Z04) and the detection of optical counterpart(s) (Z04; M05) provide a considerable amount of information on the ULX environment, available only for a very limited number of objects. Here we present a systematic study of the X-ray and optical variability of NGC 1313 X-2 based on archive data of the *XMM-Newton* satellite, and the ESO VLT and *HST* telescopes. Observations are reported in § 2 and results in § 3, where also a model for the optical emission is presented. Discussion follows.

## 2. Observations

### 2.1. X-ray observations

*XMM-Newton* observed NGC 1313 in 9 exposures taken between 2000 and 2004. All the observations are listed in Table 1. A detailed analysis of the October 2000 data of NGC 1313 X-2 have been performed by Z04 (see also Turolla et al. 2006). Here we report results from an analysis of the EPIC pn exposures of the 8 more recent observations. Data reduction and extraction have been carried out with standard software (XMM-SAS v. 6.0.0). All the observations are affected by solar flares. The good time intervals left after subtraction of the high background periods (when the total off-source count rate above 10 keV is  $> 1.0$  counts  $s^{-1}$  for EPIC pn) are reported in Table 1. For the analysis we consider all the exposures with a good time interval longer than 1 ks. After performing standard cleaning of the event lists, we extracted source counts from a circle of  $40''$  centered on the position of NGC 1313 X-2 (Z04). The background counts were extracted from a circle of  $50''$  on the same CCD.

The spectral analysis was carried out within XSPEC (v. 11.2.0). A two-component model consisting of an absorbed multicolor disk blackbody (MCD) plus a power law (PL) has been employed throughout, as it is routinely done for BHXRBs. Previous applications of the same spectral model to a number of ULXs, including NGC 1313 X-2 (Miller et al. 2003, 2004;

Cropper et al. 2004; Kong et al. 2005; Z04) gave a satisfactory fit to the data. The absorbing column density inferred from the different datasets is consistent with a constant value. We then performed again the fits fixing  $N_H$  to the average value weighted by the exposure time ( $N_H = 4.02 \times 10^{21} \text{cm}^{-2}$ ). For consistency, we also repeated the analysis of the 2000 EPIC pn spectrum of NGC 1313 X-2 following the procedure described above. The results from the spectral fits are reported in Table 2. The *XMM-Newton* fluxes were consistently derived from the parameters of the spectral fits and are reported, with the corresponding luminosities, in Table 2 (a distance of 3.7 Mpc was assumed for the host galaxy; Tully 1988). The errors have been estimated from the maximum and minimum values of the flux, obtained varying the fit parameters systematically.

## 2.2. Optical observations

B, V and R images and spectra of NGC 1313 X-2 were taken with VLT+FORs1 in December 2003. The results were presented by M05. *HST* images of this field were also obtained with ACS in two epochs (see Figure 1). The optical observations were performed in parallel with the *XMM-Newton* pointings. The observation log of the VLT and *HST* images considered here are reported in Table 1. Aperture photometry was performed on the drizzled calibrated data (reduced by the *HST* pipeline) and transformed to the Cousins system following Sirianni et al. (2005) (see Table 3).

The uncertainty on the *HST* magnitudes are dominated by the calibration error ( $\sim 0.03$  mag for the *HST* photometry of point sources), including filter transformation. As a further check of the internal consistency of the *HST* photometry, we compared the magnitudes of thirteen field stars obtained in the two epochs. The difference is significant only for one source in the sample ( $\sim 0.3$  mag). Excluding this source, the variability of which is probably intrinsic, the magnitude changes are randomly scattered around zero, with a mean absolute deviation of 0.04 mag.

The *HST* images clearly confirm that two distinct objects are present inside the X-ray error box of NGC 1313 X-2 (see Figure 1), as first shown by M05 on the basis of VLT data. If we assume  $A_V \simeq 0.3$  (Z04), taking Galactic absorption into account (the Cardelli et al. 1989 extinction law with  $R_V = A_V/E(B - V) = 3.1$  has been adopted throughout), the unreddened colors inferred from the 1st *HST* epoch are  $(B-V)_0 \sim -0.13$  and  $\sim 1.46$  for C1 and C2, respectively (see Table 3). The color for object C1 is consistent with that derived from VLT data ( $(B-V)_0 \sim -0.2$ ; M05). On the basis of the *HST* photometry, the color of object C2 is close to that of a K3-K4 supergiant. For both objects, there is evidence of variability in the V band between the two *HST* epochs ( $\sim 0.1$  mag, Figure 2; see also

Ramsey et al. 2006).

### 3. X-ray and optical variability

#### 3.1. X-ray light curve

Figure 3 shows the (unabsorbed) X-ray flux for all the available observations of NGC 1313 X-2. The *XMM-Newton* data were derived from the best fitting spectral models (see Table 2), while the *Einstein*, *ROSAT* and *ASCA* data are taken from Z04.

Until 2000 NGC 1313 X-2 exhibited variability up to a factor of two on a timescale of months, with a maximum luminosity of  $\sim 4 \times 10^{39}$  erg s $^{-1}$  (Z04). Around December 25, 2003 (observation 6 in Table 1), the source produced an intense flare, reaching a maximum unabsorbed flux of  $\sim 10.0 \times 10^{-12}$  erg cm $^{-2}$  s $^{-1}$  (Table 2). At the distance of NGC 1313 this corresponds to an intrinsic luminosity of  $\sim 10^{40}$  erg s $^{-1}$ . Clearly this value depends on the adopted spectral model and hence should be taken with care (see e.g. the slightly smaller values recently obtained for the October 2000 observation by Stobbart et al. 2006 adopting a more sophisticated spectral model). We also measured the fluxes of another ULX in the field (NGC 1313 X-3), known to be an interacting supernova (SN 1978K), in order to check if the significant luminosity increase was real or artificially produced by residual systematic effects between the two observations. The flux of the supernova ( $\sim 8.2 \times 10^{-13}$  erg cm $^{-2}$  s $^{-1}$ ) is consistent with a constant, within the uncertainties (the variation is  $\lesssim 20\%$ ). Hence we conclude that the luminosity increase of NGC 1313 X-2 is significant and fully qualifies NGC 1313 X-2 as a bright ULX.

From the observed maximum luminosity ( $L_{max} \sim 1.5 \times 10^{40}$  erg s $^{-1}$ ) and assuming isotropic emission, the black hole mass  $M_{BH}$  obtained setting  $L_{max} = L_{Edd}$  ( $L_{Edd}$  is Eddington luminosity) is  $\simeq 120M_{\odot}$ , about 2 times larger than that previously estimated by Z04. Sub-Eddington accretion would imply an even larger mass.

#### 3.2. X-ray spectral changes

The spectra of numerous ULXs, including NGC 1313 X-2, are well described by a MCD+PL model, similarly to those observed in Galactic BHXRBS. In fact, there is also some evidence of a closer similarity, inasmuch as some ULXs appear to show state transitions (Makishima et al. 2004; Winter et al. 2005). In the following we summarize the main results of an analysis of the X-ray spectral variability of NGC 1313 X-2. The most significant

result is that the slope of the PL component seems to correlate with the flux, i.e. at higher fluxes the spectrum hardens (see Table 2). This behavior was already noticed by Z04 on the basis of a comparison between two *ASCA* observations and is opposite to that usually shown by Galactic BXRBs. A similar correlation was also observed in a few ULXs in the Antennae galaxy by Fabbiano et al. (2003). The MCD component is important in the Oct 2000 and in the 2003 pointings with higher counting statistics (observations 4 and 5 in Table 1). Although there is some evidence of intrinsic variability of the thermal component, no definite conclusion can be reached at present because of the insufficient statistics. Finally, we note that the flux of the MCD component is comparable to that of the PL component (see Table 2).

### 3.3. Modeling the optical emission

In order to study the optical emission properties of objects C1 and C2 and compare them with the *HST*+*VLT* photometry, we implemented a model to compute the optical spectrum of a binary system with an IMBH taking irradiation effects into account. Our calculation relies on the same assumptions discussed in Copperwheat et al. (2005), who recently presented a thorough investigation of the infrared-through-optical emission properties of X-ray binaries with IMBHs. More specifically, we assume that accretion onto the IMBH is fuelled by a massive companion filling its Roche lobe and that the X-ray emission is isotropic; the consequences of introducing some degree of beaming are discussed later on. A standard Shakura-Sunyaev disk (e.g. Frank, King & Raine 2002) is assumed and both the X-ray irradiation of the companion (including the effects of disk shadowing) and the self-irradiation of the disk are accounted for. Following Copperwheat et al. (2005), radiative transfer at the donor and disk surfaces is treated assuming a plane-parallel atmosphere in radiative equilibrium, illuminated by the X-ray flux emitted from the innermost part of the accretion disk (see also Wu et al. 2001). In order to keep our treatment simple, the companion star is taken to be spherical, neglecting the effects produced by the Roche lobe geometry and also those related to the (possible) deformation induced by radiation pressure. Limb and gravity darkening were not included.

The model depends on the masses of the two components, the binary period (which, in turn, fixes the orbital separation), the accretion rate and the (unirradiated) temperature of the donor, in addition to the inclination angle and the orbital phase. The accretion efficiency and the albedo of the surface layers were chosen to be  $\eta = GM_{BH}/c^2 r_{in} = r_S/2r_{in} = 0.17$  (where  $r_S$  is the Schwarzschild radius and  $r_{in} = 3r_S$  is the inner disk radius) and  $\alpha = 0.9$  (e.g. de Jong, van Paradijs & Augusteijn 1996). Following Copperwheat et al. (2005), we took

the hardness ratio  $\xi = F_X(< 1.5 \text{ keV})/F_X(> 1.5 \text{ keV}) = 0.1$ . The absorption parameters in the same two spectral bands were selected as  $k_s = 2.5$  and  $k_h = 0.01$ . The V and B magnitudes of the (irradiated) disk plus donor have been computed for several values of the parameters of the binary. Each sequence of models, at fixed inclination angle  $i$ , accretion rate  $\dot{M}$  and donor mass  $M$ , corresponds to a track in the color-magnitude diagram (CMD; B-V vs. V here) along which the BH mass varies. Only inclination angles smaller than  $\sim 70^\circ$  are considered because eclipsing effects of the accretion disk on the donor (and viceversa) have not been taken into account. On the other hand, from the available data there is no positive evidence for eclipses of the X-ray source or the donor in NGC 1313 X-2. The mass and luminosity class of the donor fix its (unirradiated) surface temperature  $T_{eff}$ . Different tracks have been obtained varying the orbital period  $P_{orb}$  which, in turn, determines the Roche lobe radius. The maximum allowed period is that for which the Roche lobe radius is equal to the donor radius. The computed tracks are compared with the optical (unreddened) magnitudes and colors of objects C1 and C2 for both the VLT and *HST* observations in § 3.4.

### 3.4. Objects C1 and C2

In order to constrain the parameters of the binary, we used the optical binary emission model introduced in Section 3.3. One of the 2003 *XMM-Newton* pointings of NGC 1313 X-2 is within 2-3 days from the 1st *HST* epoch, while another is close to the VLT observation. These two *XMM-Newton* observations are those of 2003 November 25 and December 23; the latter was preferred to the observation of December 25 because of the higher statistics. It is therefore of interest to compare the V and B magnitudes of objects C1 and C2 in these two epochs. The variation of the unabsorbed X-ray flux between the same epochs is  $\sim 80\%$  (see Table 2). At the same time, however, the V and B band magnitudes of C1 do not show significant evidence of variability. The relative photometric error between the *HST* and VLT data as measured on a sample of field stars is in fact  $\simeq 0.3$  mag (see Figure 2). A similar conclusion is reached also for object C2. Again, the magnitude change between the *HST* and VLT epochs is always smaller than the relative photometric error ( $\simeq 0.5$  mag for objects fainter than V=24; see again Figure 2).

As an initial guess for the donor parameters in our model we use the values inferred on the basis of VLT photometry (M05): an O9-B0 V star of  $\sim 20M_\odot$ ,  $T_{eff} \sim 30000$  K for C1, and a G-K I star of  $\sim 10M_\odot$ ,  $T_{eff} \sim 4500$  K for C2. As mentioned above, this is consistent with what inferred from the *HST* photometry. The donor star in the case of of object C1 is assumed to be on the zero age main sequence and in contact with the Roche lobe (i.e. its radius is equal to the Roche lobe radius). Possible evolutionary effects or disturbances

caused by the intense mass transfer are not accounted for. Results for object C1 are shown in Figure 4 for two different values of  $\dot{M}$ , chosen in such a way to match the *XMM-Newton* flux measured in the two observations of 2003 November 25 and December 23. The tracks on the CMD diagram are in agreement with the observed V band magnitude and (B-V) color of object C1 for  $P_{orb} \simeq 1.7$  d,  $M \simeq 15M_{\odot}$  and  $T_{eff} \simeq 25000$  K (corresponding to an early B main sequence star). Taking into account for current uncertainties on both color and magnitude, the companion mass and temperature, and the orbital period may vary in the ranges  $10 \lesssim M/M_{\odot} \lesssim 18$ ,  $20000 \text{ K} \lesssim T_{eff} \lesssim 30000 \text{ K}$ , and  $1.5 \lesssim P_{orb} \lesssim 2$  d, respectively. If the donor makes contact with its Roche lobe and  $0.1 \lesssim M/M_{BH} \lesssim 0.8$ , the orbital period becomes a function only of the donor radius (or mass). In fact, when combining together the III Kepler’s law and the expression for the Roche lobe radius (Frank, King & Raine 2002), the dependence on  $M_{BH}$  disappears. As shown in Figure 4, the VLT and *HST* photometric points intersect the corresponding tracks at about the same value of the IMBH mass. This value increases with increasing inclination angle. Results shown in Figure 4 refer to orbital phase zero (superior conjunction). The variation in the V (B) band between the 1st *HST* epoch and the VLT one is  $\simeq 0.23$  ( $\simeq 0.25$ ), consistent (within the errors) with what observed. Thus, although in these systems X-ray irradiation is very intense, the induced optical variability is not very large owing to the high intrinsic emission of the massive B donor. The calculation for phases 0.25 and 0.5 gives results similar to those obtained for phase 0, typically within 0.15 mag. Thus, this is the expected amplitude of the modulation possibly induced by the orbital motion. It is interesting to note that this result is consistent with the degree of variability observed in the V band between the two *HST* observations ( $\sim 0.1$  mag; see Figure 2).

A direct comparison of the three cases illustrated in Figure 4 shows that relatively large values of the inclination angle ( $i \gtrsim 50^{\circ} - 60^{\circ}$ ) are required in order to obtain the correct optical flux for a BH mass  $M_{BH} \sim 120M_{\odot}$ . At lower inclination angles (top and middle panels of Figure 4), the black hole masses needed to reproduce the optical magnitudes and color of object C1 are too small for the X-ray flux to be below the Eddington limit (if the emission is isotropic). Therefore, unless the Eddington limit can be circumvented, the binary system is expected to have a significant inclination angle. We note that, for any value of  $i$ , the BH mass inferred from Figure 4 is always  $\gtrsim 70M_{\odot}$ . This absolute lower limits for  $M_{BH}$  is still compatible with a very small beaming ( $\gtrsim 0.6$ ). In this case the general picture discussed above reasonably continues to hold. On the other hand, if the ULX emission is more seriously beamed, the BH mass could be smaller: for a beaming factor  $\sim 1/6$ ,  $M_{BH}$  can be as small as  $20M_{\odot}$  without exceeding the Eddington limit. In this case, we expect no X-ray irradiation of both the disk and the companion, being the emission collimated away from the orbital plane. To test this possibility we computed a new sequence of models, following



the same procedure outlined above, but switching off the disk/donor irradiation. It turns out that it is possible to reproduce the correct magnitude and color, although the donor is now less massive and cooler. However, this implies that the star is too small to fill its Roche lobe and thus accretion can not proceed through Roche lobe overflow. Wind accretion may still be possible, although it seems unlikely that it can produce the required value of  $\dot{M}$ .

The situation for object C2 is reversed. We explored the parameter space by varying the donor mass and orbital period, but did not find any combination of values which could reproduce the data in the framework of isotropic emission. In particular, X-ray irradiation causes the (B-V) color to always exceed the observed one. On the other hand, a massive and very extended K-type supergiant ( $M \sim 16M_{\odot}$ ,  $T_{eff} \sim 4000$  K,  $P_{orb} \sim 800$  days) would have properties consistent with those of object C2 if the black hole mass is  $\sim 20M_{\odot}$ . This of course requires a (moderate) beaming. We checked that a beaming factor of  $\sim 1/6$  is enough and that the companion fills its Roche lobe. The optical magnitudes are correctly reproduced because the (unirradiated) disk contribution becomes negligible in comparison with the star intrinsic luminosity. However, in this case practically no variation in the optical is expected in response to an increase of the accretion rate, and the predicted magnitudes of C2 are constant. This is in contrast with the evidence of variability observed in the V band between the two *HST* observations ( $\sim 0.1$  mag; see Section 2.2 and Figure 2), although some variations may be induced also by the orbital ellipsoidal modulation of the donor (which we did not take into account).

#### 4. Discussion

Although present data do not allow to reach a definite conclusion on the actual counterpart of the ULX NCG 1313 X-2, some firm points may be derived from the analysis presented in the preceding sections. If C1 is the counterpart, as it seems more likely, our model indicates that this is an IMBH X-ray binary with a relatively massive main sequence donor which fills its Roche lobe. Taking a black hole mass of  $\sim 120M_{\odot}$ , as required to account for the observed X-ray flux in terms of isotropic emission, the donor mass is in the interval  $10 - 18M_{\odot}$  (taking photometric uncertainties into account, § 3.4). This is larger than the maximum main sequence mass of the parent stellar association,  $\sim 8 - 9M_{\odot}$ , estimated using multicolor photometry and isochrone fitting by Pakull, Grisé & Motch (2006) and Ramsey et al. (2006). However, considering that the lower bound for the donor mass is  $10M_{\odot}$ , the difference is small. We note also that, if C1 is the counterpart and C2 belongs to the same stellar association, the estimated masses of the two stars correctly places them on (or close to) and out of the main sequence, respectively. If the counterpart is C2 then

the source is a binary formed by a late type, massive supergiant and a stellar mass black hole with beamed X-ray emission. However, this scenario has some shortcomings. First, it predicts little if no optical variability, and this is in apparent contrast with the variations seen in the two *HST* observations. Second, the duration of the supergiant phase for a  $\sim 15M_{\odot}$  star is very short (a few  $\times 10^5$  yr), making the possibility of catching the binary in such an evolutionary stage not very likely (Patruno & Zampieri 2006). Third, the accurate astrometry of the field made possible by the cross-identification on the *Chandra* and *HST* images of a background galaxy appears to strengthen the association of NGC 1313 X-2 with object C1, ruling out object C2 (J.-F. Liu, private communication).

For object C1, an orbital modulation of amplitude  $\Delta V \sim 0.15$  is expected because of orbital inclination and X-ray irradiation effects. This modulation is superimposed to a comparable variation caused by changes in the irradiating X-ray flux ( $\sim 0.2$  mag). In this respect, it is interesting to note that similar variations in the observed B band VLT+Subaru photometry of object C1 have been recently reported also by Pakull, Grisé & Motch (2006), consistent with our findings. In principle, with a sufficient and suitably spaced number of observations, the orbital modulation can be singled out and measured with large area ground telescopes or *HST*. The detection of this modulation would lead to the unambiguous determination of the orbital period of the binary. This, in turn, would allow us to definitely discriminate between C1 and C2 and, most importantly, to constrain the mass ratio of NGC 1313 X-2 and, eventually, the mass of the black hole.

We are grateful to Claudio Germanà for his help with the binary X-ray irradiation code. We also thank an anonymous referee for useful comments that improved a previous version of this paper. We acknowledge financial contribution from contract ASI-INAF I/023/05/0 and MURST under grant PRIN-2004-023189. This paper is based on observations obtained with *XMM-Newton*, an ESA science mission with instruments and contributions directly funded by ESA Member States and NASA and on observations made with the NASA/ESA Hubble Space Telescope, obtained from the data archive at the Space Telescope Institute. STScI is operated by the association of Universities for Research in Astronomy, Inc. under the NASA contract NAS 5-26555.

## REFERENCES

- Cardelli, J.A., Clayton, G.C. & Mathis, J.S. 1989, *ApJ*, 345, 245
- Colbert, E.J.M., & Mushotzky, R.F. 1999, *ApJ*, 519, 89

- Colbert, E.J.M., & Ptak, A.F. 2002, *ApJS*, 143, 25
- Copperwheat, C., Cropper, M., Soria, R., & Wu, K. 2005, *MNRAS*, 362, 79
- Cropper, M. et al. 2004, *MNRAS*, 349, 39
- de Jong, J.A., van Paradijs, J., & Augusteijn, T. 1996, *A&A*, 314, 484
- Dewangan, G.C., Titarchuk, L., & Griffiths, R.E. 2006, *ApJ*, 637, L21
- Ebisawa, K. et al. 2003, *ApJ*, 597, 780
- Fabbiano, G. 1989, *ARA&A*, 27, 87
- Fabbiano, G. et al., 2003, *ApJ*, 584, 5
- Feng, H., & Kaaret, P. 2005, *ApJ*, 633, 1052
- Fiorito, R., & Titarchuk, L., 2004, *ApJ*, 614, L113
- Foschini, L. et al. 2002a, *A&A*, 392, 817
- Foschini, L., Ho, L.C. & Masetti, N. 2002b, *A&A*, 396, 787
- Frank, J., King, A., & Raine, D.J. 2002, *Accretion Power in Astrophysics* (Cambridge, Cambridge University Press)
- Georganopoulos, M., Aharonian, F.A., & Kirk, J.G. 2002, *A&A*, 388, L25
- Goad, M.R. et al. 2002, *MNRAS*, 335, L67
- Kaaret, P., Corbel, S., Prestwich, A.H., & Zezas, A. 2003, *Science*, 299, 365
- Kaaret, P., Ward, M.J., & Zezas, A. 2004, *MNRAS*, 351, 83
- Kaaret, P. 2005, *ApJ*, 629, 233
- Kaaret, P., Simet, M.G., & Lang, C.C. 2006a, *Science*, 311, 491
- Kaaret, P., Simet, M.G., & Lang, C.C. 2006b, *ApJ*, 646, 174
- Kawaguchi, T. 2003, *ApJ*, 593, 69
- King, A.R. et al. 2001, *ApJ*, 552, 109
- King, A.R. 2002, *MNRAS*, 335, L13

- King, A.R., & Pounds, K.A. 2003, MNRAS, 345, 657
- Kong, A.K.H., Rupen, M.P., Sjouwerman, L.O. & Di Stefano, R. 2005, in Proceedings of the XXII Texas Symposium on Relativistic Astrophysics, Stanford University, in press (astro-ph/0503465)
- Körding, E., Falcke, H. & Markoff, S. 2002, A&A, 382, L13
- La Parola, V. et al. 2001, ApJ, 556, 47
- Liu, J., Bregman, J.N., & Seitzer, P. 2002, ApJ, 580, 31
- Liu, J., Bregman, J.N., & Seitzer, P. 2004, ApJ, 602, 249
- Liu, J., & Bregman, J.N. 2005, ApJS, 157, 59
- Makishima, K. et al. 2004, AAS, 204
- Masetti, N. et al. 2003, A&A, 406, L27
- Miller, J.M., Fabbiano, G., Miller, M.C. & Fabian, A.C. 2003, ApJ, 585, L37
- Miller, J.M., Fabian, A.C. & Miller, M.C. 2004, ApJ, 607, 931
- Miller, N.A., Mushotzky, R.F., & Neff, S.G. 2005, ApJ, 623, L109
- Mucciarelli P. et al. 2005, ApJ, 633, 101 (M05)
- Mucciarelli, P. et al. 2006, MNRAS, 365, 1123
- Pakull, M.W., & Mirioni, L. 2002, in Proc. ESA Symp., New Visions of the X-ray Universe in the *XMM-Newton* and *Chandra* Era, eds. F. Jansen et al. (ESA SP-488) (astro-ph/0202488)
- Pakull, M.W., Grisé, F., & Motch, C. 2006, IAUS, 230, 293
- Patruno, A., Colpi, M., Faulkner, A., Possenti, A. 2005, MNRAS, 364, 344
- Patruno, A., Portegies Zwart, S., Dewi, J. & Hopman, C. 2006, MNRAS, 370. L6
- Patruno, A., & Zampieri, L. 2006, MNRAS, submitted
- Ramsey, C.J. et al. 2006, ApJ, 641, 241
- Roberts, T.P., & Warwick, R.S. 2000, MNRAS, 315, 98

- Roberts, T.P. et al. 2001, MNRAS, 325, L7
- Sirianni, M. et al. 2005, PASP, 117, 1049
- Soria, R. et al. 2005, MNRAS, 356, 12
- Stobbart, A.M., Roberts, T.P., Wilms, J. 2006, MNRAS, 368, 397
- Strohmayer, T.E., Mushotzky, R.F., 2003, ApJ, 586, L61
- Swartz, D.A., Ghosh, K.K., Tennant, A.F., & Wu, K. 2004, ApJS, 154, 519
- Tully, R.B. 1988, Nearby Galaxies Catalog (Cambridge: Cambridge University Press)
- Turolla, R. et al. 2006, in AdSpR, 38, 1374
- Winter, L.M., R.F. Mushotzky and C.S.Reynolds Collaboration, 2005, AAS, 207, 90.05
- Wu, K., Soria, R., Hunstead, R.W., & Johnston, H.M. 2001, MNRAS, 320, 177
- Zampieri, L. et al. 2004, ApJ, 603, 523 (Z04)

Table 1. Observation log of the *XMM-Newton* EPIC pn pointings and of the VLT+FORs1 and *HST*+ACS photometric observations of NGC 1313 X-2.

|   | Instrument                | Obs. Id.   | Date       | Exposure | GTI <sup>a</sup> | Filter |
|---|---------------------------|------------|------------|----------|------------------|--------|
| 1 | <i>XMM-Newton</i> EPIC pn | 0106860101 | 2000-10-17 | 31637s   | 20600s           | Medium |
| 2 | <i>XMM-Newton</i> EPIC pn | 0150280101 | 2003-11-25 | 8365s    | 1087s            | Thin   |
| 3 | <i>XMM-Newton</i> EPIC pn | 0150280201 | 2003-12-09 | 5620s    | 0s               | Thin   |
| 4 | <i>XMM-Newton</i> EPIC pn | 0150280301 | 2003-12-21 | 10334s   | 8272s            | Thin   |
| 5 | <i>XMM-Newton</i> EPIC pn | 0150280401 | 2003-12-23 | 14094s   | 3600s            | Thin   |
| 6 | <i>XMM-Newton</i> EPIC pn | 0150280501 | 2003-12-25 | 15282s   | 1668s            | Thin   |
| 7 | <i>XMM-Newton</i> EPIC pn | 0150280701 | 2003-12-27 | 16666s   | 0s               | Thin   |
| 8 | <i>XMM-Newton</i> EPIC pn | 0150280601 | 2004-01-08 | 14756s   | 7696s            | Thin   |
| 9 | <i>XMM-Newton</i> EPIC pn | 0150281101 | 2004-01-16 | 7034s    | 4208s            | Thin   |
|   | VLT+FORs1                 |            | 2003-12-24 | 840×2    |                  | B      |
|   | VLT+FORs1                 |            | 2003-12-25 | 600×2    |                  | V      |
|   | <i>HST</i> +ACS(I epoch)  |            | 2003-11-22 | 580×2    |                  | F555w  |
|   | <i>HST</i> +ACS           |            | 2003-11-22 | 630×4    |                  | F435w  |
|   | <i>HST</i> +ACS(II epoch) |            | 2004-02-22 | 600×4    |                  | F555w  |

<sup>a</sup>Good Time Intervals in which the total off-source count rate above 10 keV is  $< 1.0$  counts  $s^{-1}$ .

Table 2. Spectral analysis of *XMM-Newton* EPIC pn data of NGC 1313 X-2.<sup>a</sup>

|   | Date       | Count rate | Flux <sup>b</sup>      | $F_{MCD}/F_{PL}$ <sup>c</sup> | $L$ <sup>d</sup>         | $kT_{MCD}$ [keV]       | $\Gamma$            | $\chi^2_{red}/d.o.f.$ |
|---|------------|------------|------------------------|-------------------------------|--------------------------|------------------------|---------------------|-----------------------|
| 1 | 2000-10-17 | 0.24       | $4.00^{+0.82}_{-0.62}$ | 0.93                          | $6.52^{+1.34}_{-1.02}$   | $0.16^{+0.02}_{-0.01}$ | $2.3^{+0.1}_{-0.1}$ | 1.24/75               |
| 2 | 2003-11-25 | 0.67       | $5.07^{+0.23}_{-0.18}$ | –                             | $8.30^{+0.04}_{-22.0}$   | –                      | $2.3^{+0.2}_{-0.2}$ | 1.06/44               |
| 4 | 2003-12-21 | 0.80       | $9.46^{+1.55}_{-1.65}$ | 0.63                          | $15.43^{+2.53}_{-2.69}$  | $0.13^{+0.01}_{-0.02}$ | $1.9^{+0.1}_{-0.1}$ | 1.11/144              |
| 5 | 2003-12-23 | 0.89       | $9.19^{+3.10}_{-1.74}$ | 0.94                          | $14.99^{+5.06}_{-2.84}$  | $0.15^{+0.03}_{-0.03}$ | $1.8^{+0.1}_{-0.1}$ | 0.99/140              |
| 6 | 2003-12-25 | 0.56       | $10.0^{+8.80}_{-3.85}$ | 0.87                          | $16.31^{+14.36}_{-6.28}$ | $0.15^{+0.04}_{-0.04}$ | $2.1^{+0.2}_{-0.2}$ | 0.99/42               |
| 8 | 2004-01-08 | 0.39       | $5.63^{+2.97}_{-1.00}$ | 0.47                          | $9.18^{+4.84}_{-1.63}$   | $0.13^{+0.03}_{-0.02}$ | $2.5^{+0.1}_{-0.1}$ | 0.82/67               |
| 9 | 2004-01-16 | 0.34       | $4.38^{+1.01}_{-1.12}$ | 0.45                          | $7.14^{+1.65}_{-1.83}$   | $0.17^{+0.02}_{-0.03}$ | $2.3^{+0.1}_{-0.1}$ | 1.01/66               |

<sup>a</sup> $N_H$  has been frozen at  $4.02 \times 10^{21} \text{ cm}^{-2}$

<sup>b</sup>Unabsorbed flux in units of  $10^{-12} \text{ erg cm}^{-2} \text{ s}^{-1}$

<sup>c</sup>Ratio of the (unabsorbed) fluxes of the MCD and PL components.

<sup>d</sup>Unabsorbed luminosity, in units of  $10^{39} \text{ erg s}^{-1}$ , for a distance of 3.7 Mpc

Table 3. Observed magnitudes and colors of the two candidate optical counterparts of NGC 1313 X-2.

|                     | Filter | C1         | C2         |
|---------------------|--------|------------|------------|
| <i>HST</i> I epoch  | B      | 23.72±0.04 | 26.02±0.04 |
| VLT                 | B      | 23.50±0.15 | ≥ 25.2     |
| <i>HST</i> I epoch  | V      | 23.75±0.04 | 24.46±0.04 |
| VLT                 | V      | 23.60±0.15 | 24.10±0.15 |
| <i>HST</i> II epoch | V      | 23.61±0.04 | 24.57±0.04 |
| <i>HST</i> I epoch  | B-V    | -0.03±0.06 | 1.56±0.06  |
| VLT                 | B-V    | -0.1±0.2   | ≥ 1.1      |

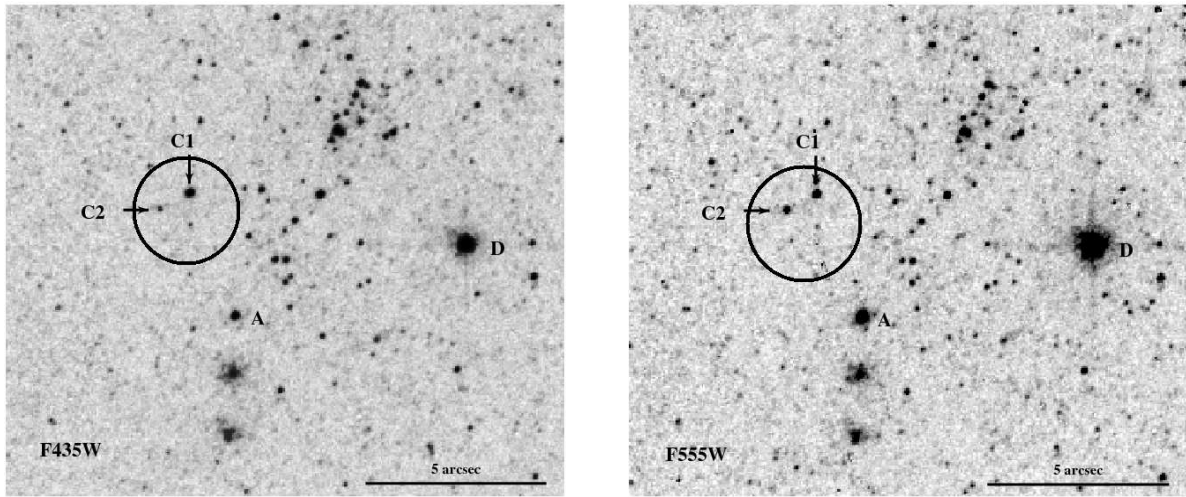


Fig. 1.— *HST*+*ACS* images of NGC 1313 X-2: left F435W (B) band, right F555W (V) band. The *Chandra* error box, the candidate optical counterparts C1 and C2 and the field sources A and D are shown (following Z04 and M05).



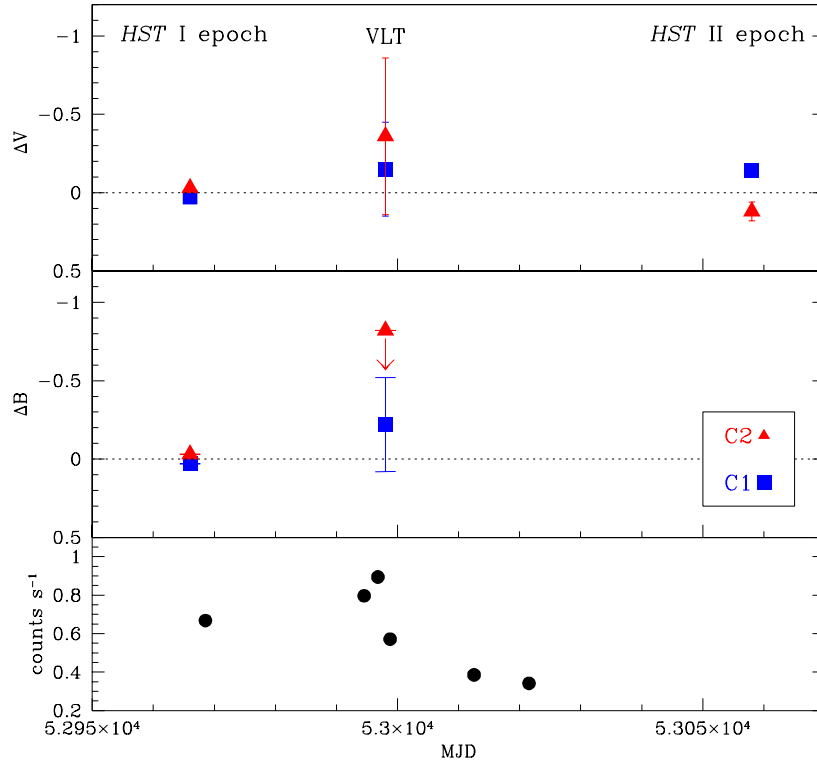


Fig. 2.— *Top and middle panels:*  $\Delta V = V - V(\text{HST I epoch})$  and  $\Delta B = B - B(\text{HST I epoch})$  for objects C1 and C2 for the available epochs. The error bars correspond to 0.3 and 0.5 mag for V and B respectively (see text for details). *Lower panel:* XMM-Newton count rates of NGC 1313 X-2 in the [0.2-10.0] keV range.

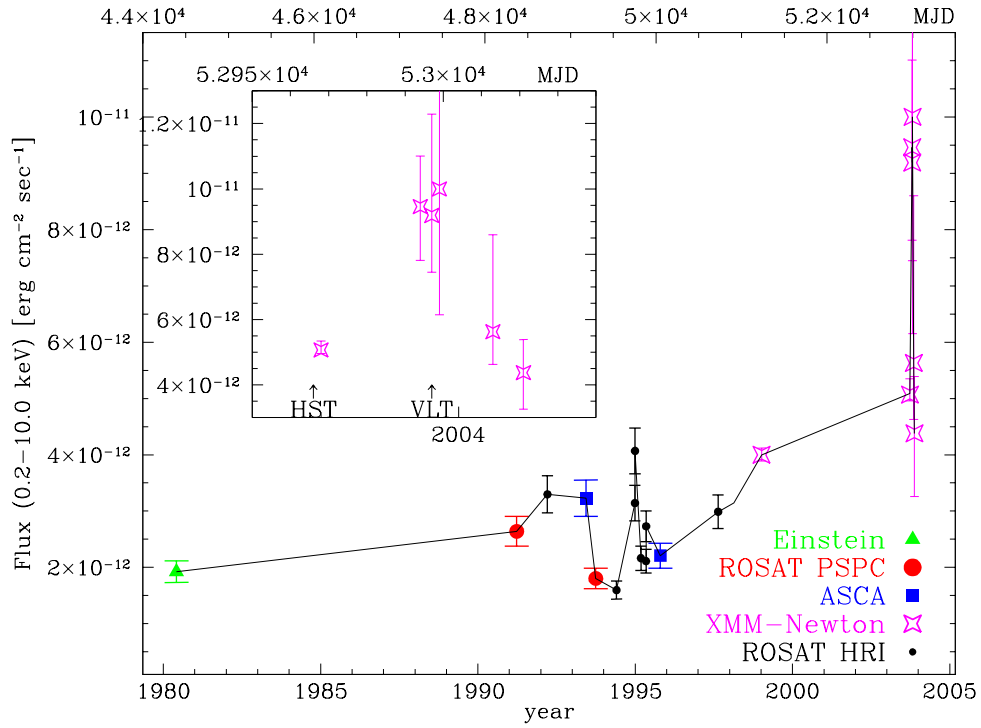


Fig. 3.— The X-ray lightcurve of NGC 1313 X-2. Fluxes are unabsorbed and refer to the [0.2–10.0] keV energy interval (see Table 2). *Einstein*, *ROSAT* and *ASCA* points are taken from Z04. The insert refers to the more recent *XMM-Newton* data (Table 2) and the arrows mark the time of the *HST* and *VLT* observations (Table 1).

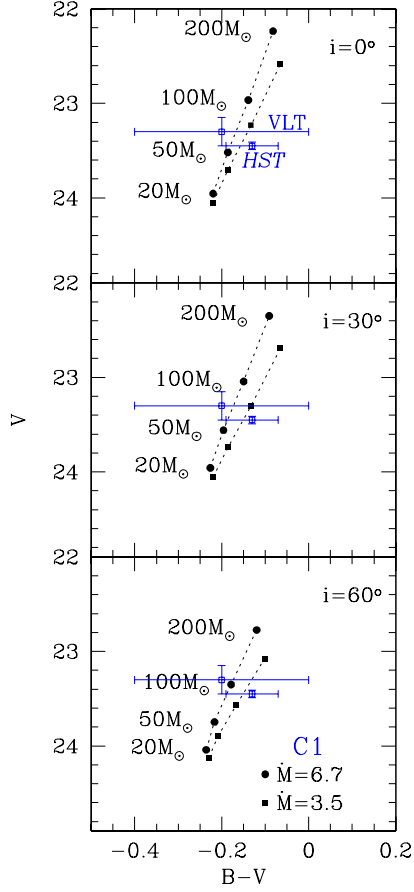


Fig. 4.— Color-magnitude diagram for the (irradiated) disk plus donor model for  $P_{orb} \simeq 1.7$  d,  $M \simeq 15M_{\odot}$  and  $T_{eff} \simeq 25000$  K (object C1). Each panel refers to a different inclination angle  $i$ . The two tracks correspond to  $\dot{M} = 3.5$  and  $6.7 \dot{M}_{Edd}$ . These values are chosen in such a way to match the *XMM-Newton* flux measured in the two observations of 2003 November 25 and December 23, that are quasi-simultaneous to the *HST* I epoch and VLT observations, respectively. The labels indicate the BH mass. The V magnitude and B-V color as obtained from the VLT and the *HST* observations are also shown (*open squares*).